ACS APPLIED MATERIALS & INTERFACES

Research Article

www.acsami.org

Electrochemical Oxidation of Hydrolyzed Poly Oxymethylene-dimethyl Ether by PtRu Catalysts on Nb-Doped $SnO_{2-\delta}$ Supports for Direct Oxidation Fuel Cells

Katsuyoshi Kakinuma,*[,†] In-Tae Kim,[†,§] Yuichi Senoo,[†,‡] Hiroshi Yano,[†] Masahiro Watanabe,*[,†] and Makoto Uchida*[,†]

[†]Fuel Cell Nanomaterials Center, University of Yamanashi, Miyamae 6-43, Kofu 400-0021, Japan

[‡]Mitsui Mining and Smelting Co., Ltd., Haraichi 1333-2, Ageo, Saitama 362-0021, Japan

Supporting Information

ABSTRACT: We synthesized Pt and PtRu catalysts supported on Nb-doped $SnO_{2-\delta}$ ($Pt/Sn_{0.99}Nb_{0.01}O_{2-\delta}$, $PtRu/Sn_{0.99}Nb_{0.01}O_{2-\delta}$) for direct oxidation fuel cells (DOFCs) using poly oxymethylene-dimethyl ether (POMM*n*, *n* = 2, 3) as a fuel. The onset potential for the oxidation of simulated fuels of POMM*n* (methanol-formaldehyde mixtures; *n* = 2, 3) for $Pt/Sn_{0.99}Nb_{0.01}O_{2-\delta}$ and $PtRu/Sn_{0.99}Nb_{0.01}O_{2-\delta}$ was less than 0.3 V vs RHE, which was much lower than those of two commercial catalysts (PtRu black and Pt_2Ru_3/carbon black). In particular, the onset potential of the oxidation reaction of simulated fuels of POMM*n* (*n* = 2, 3) for $PtRu/Sn_{0.99}Nb_{0.01}O_{2-\delta}$ sintered at 800 °C in nitrogen atmosphere was less than 0.1 V vs RHE and is thus considered to be a promising anode catalyst for DOFCs. The mass activity (MA) of $PtRu/Sn_{0.99}Nb_{0.01}O_{2-\delta}$ sintered at 800 °C was more than five times larger than those of the commercial catalysts in the measurement temperature range from 25 to 80 °C. Even though the MA for the methanol oxidation reaction was of the same order as those of the commercial catalysts, the MA for the formaldehyde oxidation reaction was more than five times larger than those of the commercial catalysts. Sn from the $Sn_{0.99}Nb_{0.01}O_{2-\delta}$ support was found to have diffused into the Pt catalyst during the sintering process. The Sn on the top surface of the Pt catalyst accelerated the oxidation of carbon monoxide by a bifunctional mechanism, similar to that for Pt−Ru catalysts.

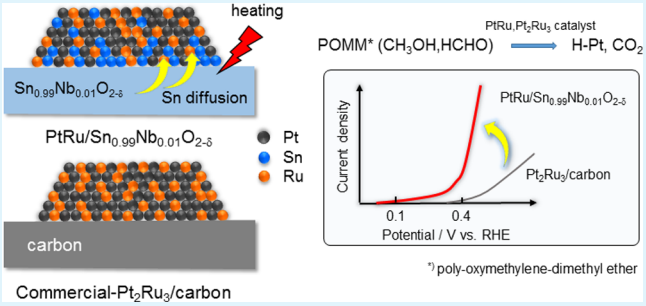

KEYWORDS: *direct oxidation fuel cell, anode, hydrolyzed poly oxymethylene-dimethyl ether (POMM), Nb-doped $SnO_{2-\delta}$ support, PtRu catalyst*

INTRODUCTION

Polymer electrolyte fuel cells (PEFCs) fueled directly with liquid fuels are promising candidates for application as portable power sources such as mobile phones, personal digital assistants (PDAs), and laptop computers.[1,2] Liquid alcohol fuels such as methanol, ethanol, and propanol have several advantages, including good energy density and low cost.[3−8] However, alcohol-fueled PEFCs have been slow to be commercialized. One of the main problems is that portable use involves safety issues. These alcohol fuels have low flash points, below room temperature, as well as toxicity. The transportable quantities and methodology of transporting liquid fuels are restricted under regulations, although these have been relaxed recently, specifically for air travel. An alternative fuel type that has also been considered is the family of poly oxymethylene-dimethyl ethers (POMM*n*: $CH_3-O-(CH_2-O)_n-CH_3$, *n* = 1−8), which are liquid oligomers at room temperature, with less toxicity and higher flash points (>64 °C).[9] During actual usage, they are easily hydrolyzable to methanol and formaldehyde under acidic conditions (eq 1)

$$CH_3 - O - (CH_2 - O)_n - CH_3 + H_2O \rightarrow 2CH_3OH + nHCHO \quad (1)$$

Our group reported that the hydrolysis of POMM*n* on platinum-based catalysts occurred easily in a 0.1 mol dm^{-3} $HClO_4$ solution and that these oligomers have the potential to be considered as safe alternative liquid fuels.[10,11]

During the oxidation of the hydrolysis products, methanol, and formaldehyde, the intermediate carbon monoxide (CO) is produced, which is a well-known poison on the platinum surface. The prevention of CO poisoning on the Pt anode surface is required in order to use PEFCs fueled directly with these and other well-known liquid fuels. The use of alloys with a second or a third metal, such as PtRu and PtSn, etc., is expected to lead to CO tolerance based on the bifunctional theory; these

Received: August 18, 2014
Accepted: November 21, 2014
Published: November 21, 2014

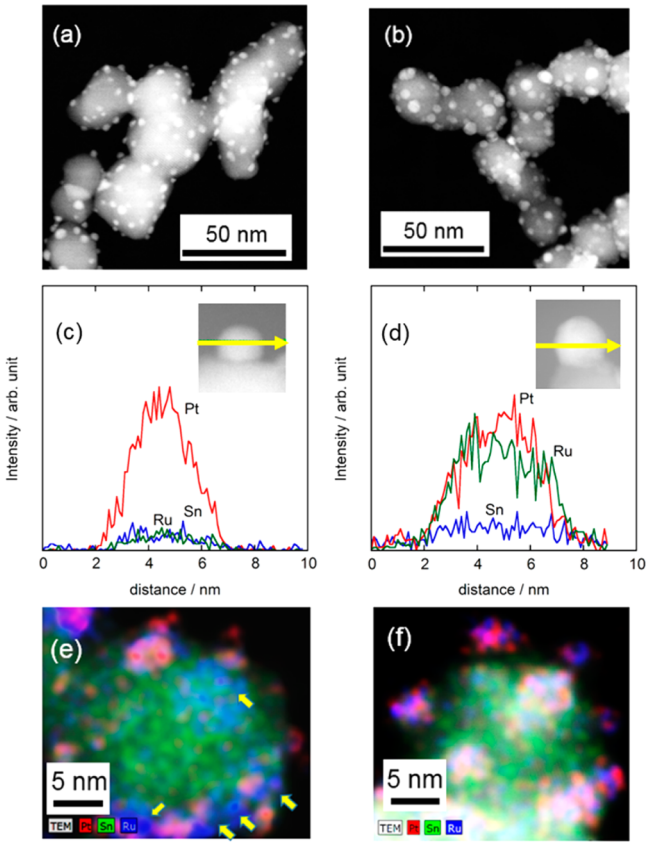

Figure 1. STEM-EDX analysis of PtRu/$Sn_{0.99}Nb_{0.01}O_{2-\delta}$ catalysts. (a, b) HAADF-STEM images of PtRu/$Sn_{0.99}Nb_{0.01}O_{2-\delta}$ sintered at 600 and 800 °C under nitrogen atmosphere. (c, d) Line profiles of elements in noble metal of PtRu/$Sn_{0.99}Nb_{0.01}O_{2-\delta}$ catalyst sintered at 600 and 800 °C under nitrogen atmosphere. Inseted images denote the line profile position. (e, f) Elemental mapping of PtRu/$Sn_{0.99}Nb_{0.01}O_{2-\delta}$ sintered at 600 and 800 °C under nitrogen atmosphere. Yellow arrows denote the localization of Ru.

are preferred candidate catalysts for PEFCs fueled directly with liquid fuels.[12−24]

In this paper, we focused on colloid-deposited Pt and PtRu catalysts supported on the aggregated nanometer-sized Nb-doped $SnO_{2-\delta}$, including the fusion of nearest-neighbor support particles to form a random branching structure, for application in PEFCs fueled directly with liquid POMM*n* (*n* = 2, 3). We characterized the catalysts by XRD, STEM-EDX, and XPS, and evaluated their anodic performance with simulated fuels of POMM*n* (*n* = 2, 3), methanol, and formaldehyde by a channel flow cell at various temperatures.

EXPERIMENTAL SECTION

Preparation of Catalysts. The $Sn_{0.96}Nb_{0.04}O_{2-\delta}$ nanosized particles with aggregated network structure for use as PtRu and Pt catalyst supports were synthesized by the flame oxide synthesis method; details of the method are described in earlier papers.[25−27] The as-prepared oxide was sintered at 800 °C for 2 h in air in a rotary kiln furnace. Single phases of these oxides were detected by X-ray diffraction measurements (XRD, Ultima 4, Rigaku Co.) with Cu Kα radiation (0.15406 nm, 40 kV, 40 mA). The surface area of the $Sn_{0.99}Nb_{0.01}O_{2-\delta}$ support was 37 $m^2\ g^{-1}$, estimated by the Brunauer−Emmett−Teller adsorption method (BET, BELSORP-max, Nippon BEL Co.). We supplied the $Sn_{0.99}Nb_{0.01}O_{2-\delta}$ support to Tanaka Kikinzoku Kogo K. K, which then carried out the metal loading to produce the PtRu/$Sn_{0.99}Nb_{0.01}O_{2-\delta}$ and Pt/$Sn_{0.99}Nb_{0.01}O_{2-\delta}$ catalysts.

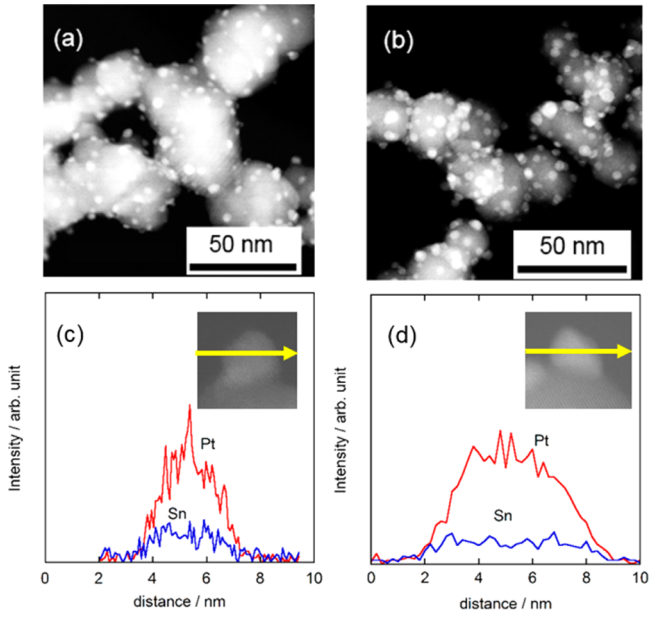

Figure 2. STEM-EDX analysis of PtRu/$Sn_{0.99}Nb_{0.01}O_{2-\delta}$ catalysts. (a, b) HAADF-STEM images of Pt/$Sn_{0.99}Nb_{0.01}O_{2-\delta}$ sintered at 600 and 800 °C under nitrogen atmosphere. (c, d) Line profiles of elements in Pt/$Sn_{0.99}Nb_{0.01}O_{2-\delta}$ sintered at 600 and 800 °C under nitrogen atmosphere. Inseted images denote the line profile position.

(PtRu/$Sn_{0.99}Nb_{0.01}O_{2-\delta}$: Pt loading 7.8 wt %, Ru loading 3.5 wt %). The Pt nanoparticles were loaded on the support by a colloidal method (Pt/$Sn_{0.99}Nb_{0.01}O_{2-\delta}$: Pt loading 8.7 wt %). Each catalyst was heat-treated at 600 and 800 °C in nitrogen gas for 2 h and then quenched at room temperature in the same atmosphere. Commercial PtRu black (TEC90110: Pt loading 60.3 wt %, Ru loading 31.2 wt %) and Pt_2Ru_3/carbon black (Pt_2Ru_3/CB: TEC81E81: Pt loading 41.7 wt %, Ru loading 32.4 wt %, CB surface area 800 m^2g^{-1}) were supplied by Tanaka Kikinzoku Kogo K. K.

The particle size distributions of Pt and microstructures of the catalysts thus obtained were characterized by images from transmission electron microscopy (TEM, H-9500, Hitachi High Technologies Co.) and images of high-angle annular dark field scanning transmission electron microscopy (HAADF-STEM) images from a scanning transmission electron microscope (STEM, HD-2700, Hitachi High Technologies Co.) with an energy-dispersive X-ray spectroscopic attachment (EDX, Quantax XFlash 5010, Bruker AXS K.K.). The electronic states of the component elements were characterized with X-ray photoelectron spectroscopy (XPS, JPS-9010, JEOL Ltd.) with in situ heat treatment equipment.

Electrochemical Measurements. We evaluated the effect of PtRu/$Sn_{0.99}Nb_{0.01}O_{2-\delta}$, Pt/$Sn_{0.99}Nb_{0.01}O_{2-\delta}$, and commercial catalysts (PtRu black and Pt_2Ru_3/CB) on the electrochemical oxidation of POMM*n* (*n* = 2, 3), formaldehyde and methanol by use of a multichannel flow double electrode (M-CFDE) cell. Details of the M-CFDE cell used are described in our previous papers.[28,29] Each catalyst was maintained at 0.05 V for 30 min in CO-saturated 0.1 M $HClO_4$ solution to ensure that the Pt sites were sufficiently covered by CO. Then, a CO stripping measurement was conducted in N_2-saturated 0.1 M $HClO_4$ solution (CO-free condition) at 20 mV s^{-1} to oxidize the adsorbed CO (CO_{ads}) on the working electrode. We have found that the hydrolyzed POMM*n* (*n* = 1−8) fuels are oxidized much more quickly than the original, unhydrolyzed ones,[11] and proposed a direct fuel cell system combined with a prehydrolysis stage by acid catalysis.[10] On the basis of such previous works, we used here "simulated fuels" of mixtures of methanol and formaldehyde as convenient models for the 100% hydrolyzed fuels of 0.30 M $POMM_2$ and 0.25 M $POMM_3$, which is equivalent to 1.00 M CH_3OH in the electric charges for their complete oxidation, i.e., 0.60 M CH_3OH + 0.60 M HCHO and 0.50 M CH_3OH + 0.75 M HCHO, respectively. As the reference fuels, we also used 1.00 M

Table 1. Atomic Ratios of the Metal Catalyst Nanoparticles, Pt Particle Size, Particle Size of Noble Metal, and Electrochemical Surface Area of Each Catalyst

sample	sintered temperature (°C)	atomic ratios of the metal catalyst nanoparticles[a] Pt	Ru	Sn	particle size of noble metal (nm)	electrochemical active surface area estimated from CO stripping $ECSA_{CO}$ ($m^2\ g^{-1}$)
$PtRu/Sn_{0.96}Nb_{0.01}O_{2-\delta}$	600	0.60	0.25	0.15	2.98 ± 0.70	68.8
$PtRu/Sn_{0.96}Nb_{0.01}O_{2-\delta}$	800	0.43	0.38	0.19	5.24 ± 1.44	67.3
$Pt/Sn_{0.96}Nb_{0.01}O_{2-\delta}$	600	0.85		0.15	3.73 ± 0.44	90.2
$Pt/Sn_{0.96}Nb_{0.01}O_{2-\delta}$	800	0.84		0.16	5.90 ± 1.21	63.1
Pt_2Ru_3/CB					2.05 ± 0.44	
PtRu					3.00 ± 0.55	

[a]Atomic ratios of the metal catalyst nanoparticles are based on spot analyses of more than 20 particles, with the electron beam focused on each particle (ca. 2−6 nm), so that the atomic ratios reflect only the catalyst particles (Figure 1S in the Supporting Information).

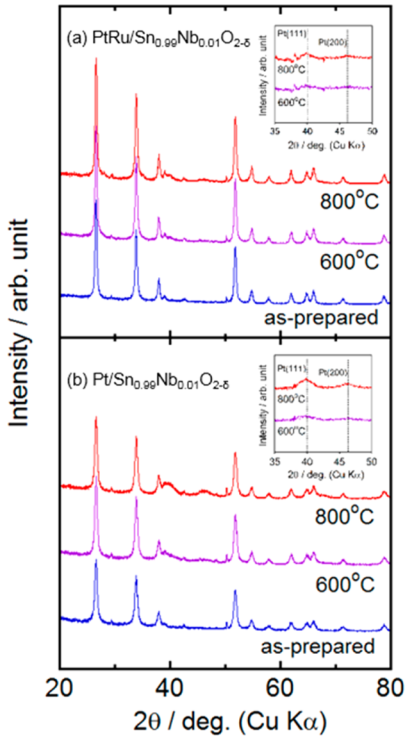

Figure 3. (a) XRD patterns of $PtRu/Sn_{0.99}Nb_{0.01}O_{2-\delta}$ catalysts and (b) $Pt/Sn_{0.99}Nb_{0.01}O_{2-\delta}$ catalyst. Inseted profiles are differential XRD profiles of $PtRu/Sn_{0.99}Nb_{0.01}O_{2-\delta}$ and $Pt/Sn_{0.99}Nb_{0.01}O_{2-\delta}$ against $Sn_{0.99}Nb_{0.01}O_{2-\delta}$ support sintered at 600 and 800 °C under nitrogen atmosphere.

CH_3OH and 1.50 M HCHO in the evaluation of oxidation performances at the newly developed catalysts. From the hydrodynamic voltammograms at various temperatures of the O_2-saturated electrolyte solutions, we calculated the kinetically controlled electrochemical oxidation activity for simulated POMM*n* (*n* = 2, 3), as well as pure formaldehyde and methanol, at the working electrode. On each working electrode, the various catalysts mentioned above were uniformly dispersed on an Au working electrode (flow direction length 1 mm, width 4 mm, geometric area 0.04 cm^2) at a constant loading of platinum, 5.5 $\mu g\ cm^{-2}$. Nafion films were cast on the catalyst layer with an average film thickness of 0.1 μm.[30] The Nafion-coated catalysts on gold were heated at 130 °C for 30 min in air to adhere the Nafion to the catalyst. A platinum mesh was used as the counter electrode. All electrode potentials were controlled by an 8-channel multipotentiostat (HA1010 mM8, Hokuto Denko Co., Japan) with respect to the reversible hydrogen electrode (RHE). The RHE, which was maintained at the same temperature as that of the cell (*t*, °C) [denoted as RHE(*t*)], was used as the reference electrode. The flow circuit system of the electrolyte solution used was the same as that described previously.[28,29] The electrolyte solution of 0.1 M $HClO_4$ was prepared from reagent grade chemicals (Kanto Chemical Co., Japan) and Milli-Q water (Milli-Pore Japan Co., Ltd.) and purified in advance by conventional pre-electrolysis methods.[31] The electrolyte solution was saturated with N_2 or O_2 gas bubbling for at least 1 h prior to the electrochemical measurements. The electrolyte flow rate was 30 $cm\ s^{-1}$.

RESULTS AND DISCUSSION

Characterization of $PtRu/Sn_{0.99}Nb_{0.01}O_{2-\delta}$ and $Pt/Sn_{0.99}Nb_{0.01}O_{2-\delta}$. HAADF-STEM images of $PtRu/Sn_{0.99}Nb_{0.01}O_{2-\delta}$ and $Pt/Sn_{0.99}Nb_{0.01}O_{2-\delta}$ sintered at 600 and 800 °C under nitrogen are shown in Figure 1a, b and Figure 2a, b. Each of the support nanoparticles are fused partially with nearest neighbors, forming a randomly branched structure. This branched structure has continuous chains of necked particles with low contact resistance, which act as electronically conductive paths.[27,32,33] This structure also forms open pores from 10 to 50 nm in diameter. We consider that the open pores act as mass transport paths for reactants such as oxygen and hydrogen, fuels such as methanol and formaldehyde, as well as POMM*n* (*n* = 2, 3). Such pores should be suitable for gas diffusion electrodes in PEFCs. The noble metal catalyst particles were dispersed uniformly on the support with hemispherical shape, and the particle sizes were well controlled as listed in Table 1. The chemical compositions of each catalyst, which were characterized by spot analysis of STEM-EDX (spot size 0.2 nm), are also listed in Table 1 (see Figure 1S in the Supporting Information). We found that each of the catalysts contained Sn, suggesting that they had reacted with the $Sn_{0.99}Nb_{0.01}O_{2-\delta}$ support during the sintering procedure.

The distributions of each element in these catalysts were also characterized by STEM-EDX line analysis. The $PtRu/Sn_{0.99}Nb_{0.01}O_{2-\delta}$ and $Pt/Sn_{0.99}Nb_{0.01}O_{2-\delta}$ catalysts sintered at 600 °C (Figures 1c and 2c) showed that the Sn and Ru content around the surfaces of the particles were relatively lower than that of the central area. We conclude that the surfaces of the catalyst particles sintered at 600 °C were covered with a Pt-rich phase. The catalysts sintered at 800 °C (Figures 1d and 2d) showed that each element was uniformly distributed in the catalyst particle, and that portions of both Sn and Ru were exposed on the top surface. As shown in the STEM-EDX mapping (Figure 1e), part of the Ru metal (localized blue area indicated with yellow arrow) was localized on the support after sintering at 600 °C. After sintering at 800 °C, the STEM-EDX mapping of Figure 1(f) showed that the localized Ru metal were not observed, and the catalyst composition was close to the desired ratio (Pt:Ru = 1:1).

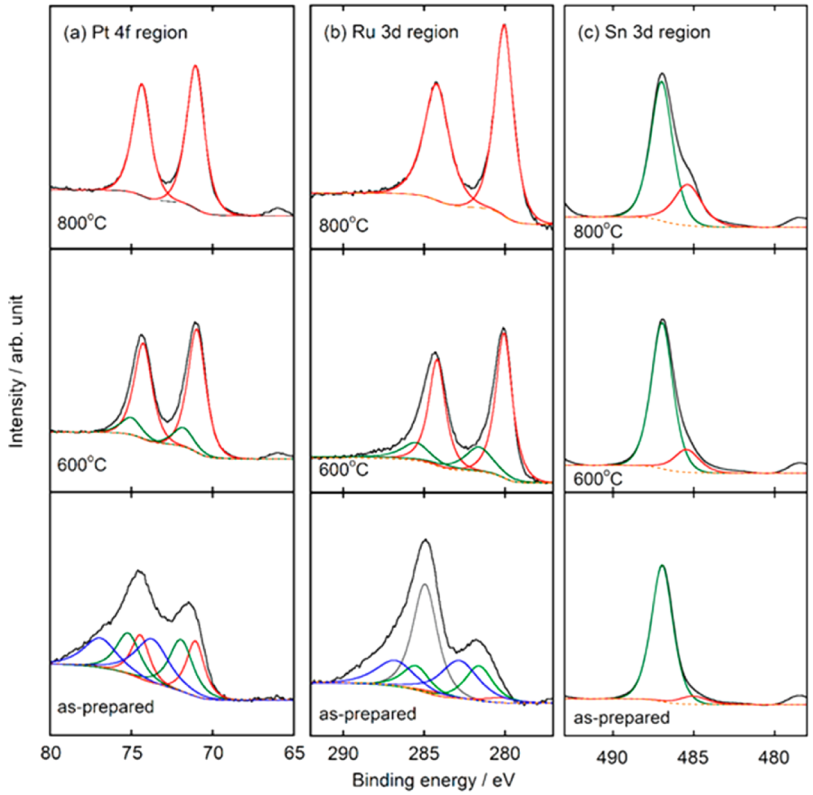

Figure 4. XPS spectra of Pt 4f, Ru 3d, and Sn 3d regions for as-prepared PtRu/$Sn_{0.99}Nb_{0.01}O_{2-\delta}$ catalyst and the catalysts sintered at 600 and 800 °C under nitrogen atmosphere. The spectra were deconvoluted based on NIST reference spectra.[34] (a) black line, raw data; red line, Pt metal; green line, PtO; blue line, PtO_2; (b) black line, raw data; red line, Ru metal; green line, RuO_2; blue line, RuO_3; gray line, carbon; (c) black line, raw data; red line, Sn metal; green line, SnO_2.

The XRD patterns of both PtRu/$Sn_{0.99}Nb_{0.01}O_{2-\delta}$ and Pt/$Sn_{0.99}Nb_{0.01}O_{2-\delta}$ after sintering at 600 and 800 °C under nitrogen are shown in Figure 3a, b. The inseted figures were differential XRD profile of PtRu/$Sn_{0.99}Nb_{0.01}O_{2-\delta}$ and Pt/$Sn_{0.99}Nb_{0.01}O_{2-\delta}$ against $Sn_{0.99}Nb_{0.01}O_{2-\delta}$ support. The XRD profiles showed that the peaks around 2θ = 39.5° originated from some peaks including Pt, PtRu, PtSn, and any other Pt−Ru−Sn alloys; these grew with increasing sintering temperature because of increasing crystallite sizes of the catalysts.

XPS spectra of the as-prepared and sintered catalysts (600 °C, 800 °C) are shown in Figures 4 and 5. More than 50 atom % of the Pt in the as-prepared PtRu/$Sn_{0.99}Nb_{0.01}O_{2-\delta}$ and Pt/$Sn_{0.99}Nb_{0.01}O_{2-\delta}$ catalysts was in the oxide state (Figure 4a, b). After sintering at 800 °C in nitrogen atmosphere, all of the Pt converted to Pt metal. Similar behavior occurred with the Pt/$Sn_{0.99}Nb_{0.01}O_{2-\delta}$ catalyst. More than 90 atom % of the Ru in the as-prepared PtRu/$Sn_{0.99}Nb_{0.01}O_{2-\delta}$ catalyst was in the oxide state (Figure 4b). After the sintering procedure at 800 °C in nitrogen atmosphere, the Ru in the PtRu/$Sn_{0.99}Nb_{0.01}O_{2-\delta}$ catalyst also changed to the Ru metal state. Both PtRu/$Sn_{0.99}Nb_{0.01}O_{2-\delta}$ and Pt/$Sn_{0.99}Nb_{0.01}O_{2-\delta}$ catalysts contain Sn metal state, which originated from the $Sn_{0.96}Nb_{0.01}O_{2-\delta}$ support (Figures 4c and 5b). However, we also found that the Sn metal appeared clearly in the PtRu/$Sn_{0.99}Nb_{0.01}O_{2-\delta}$ catalyst after sintering at 800 °C in nitrogen atmosphere. The Sn metal peak also appeared in the Pt/$Sn_{0.99}Nb_{0.01}O_{2-\delta}$ catalyst, but the peak intensity was small.

From these results, we summarize the characterization of the catalysts on the $Sn_{0.99}Nb_{0.01}O_{2-\delta}$ support below. The results are also shown schematically in Figure 6. Each catalyst was a disordered alloy including Sn, with hemispherical particles in the 3−6 nm range, and they were uniformly dispersed on the $Sn_{0.99}Nb_{0.01}O_{2-\delta}$ support. The surfaces of the PtRu catalyst particles after sintering at 600 °C consisted mainly of Pt metal and only slightly of Ru metal, Sn metal, and Ru oxides. After sintering at 800 °C, the surface concentrations of Sn metal on the PtRu particles increased sharply, together with that of Ru metal. In the case of the Pt catalyst, similar behavior occurred, but the concentration of metallic Sn was relatively small.

Electrochemical Characterization of PtRu/$Sn_{0.99}Nb_{0.01}O_{2-\delta}$ and Pt/$Sn_{0.99}Nb_{0.01}O_{2-\delta}$. Figure 7 shows the adsorbed CO stripping voltammograms for each catalyst in 0.1 mol dm^{-3} $HClO_4$ solution saturated with N_2 at 25 °C. The onset of CO_{ads} oxidation was observed at 0.36 V vs RHE on both Pt/$Sn_{0.99}Nb_{0.01}O_{2-\delta}$, at 0.42 V vs RHE on Pt/$Sn_{0.99}Nb_{0.01}O_{2-\delta}$ sintered at 600 °C, and at 0.34 V on PtRu/$Sn_{0.99}Nb_{0.01}O_{2-\delta}$ sintered at 800 °C, all of which were lower than that of Pt/C. These results indicate the promotion effect of the CO_{ads} oxidation by the alloying of Sn and Ru.

The electrochemically active surface areas of all samples, estimated from the CO stripping peak areas ($ECSA_{CO}$), are listed in Table 1. The CO stripping peak potential is sensitive to the PtRu surface. The $ECSA_{CO}$ of PtRu/$Sn_{0.99}Nb_{0.01}O_{2-\delta}$ sintered at 600 °C was lower than that of Pt/$Sn_{0.99}Nb_{0.01}O_{2-\delta}$ sintered at 600 °C, which would correspond to the effect of Ru coverage on the catalyst surface. After the sintering procedure at 800 °C, Sn and Ru were uniformly distributed in the catalyst particles, as shown in the STEM-EDX mapping (Figures 1d and 2d). We consider that similar amounts of Sn and Ru were

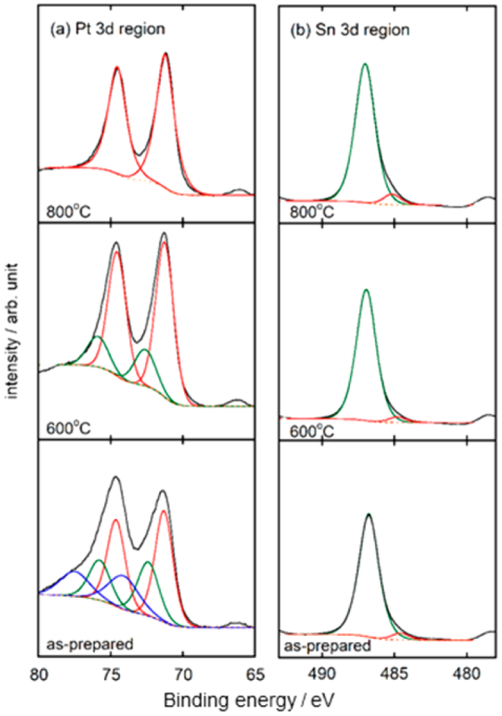

Figure 5. XPS spectra of Pt 4f and Sn 3d region for as prepared $Pt/Sn_{0.99}Nb_{0.01}O_{2-\delta}$ catalyst and the catalysts sintered at 600 and 800 °C under nitrogen atmosphere. The spectra were also deconvoluted based on NIST reference spectra.[34] (a) Black line, raw data; red line, Pt metal; green line, PtO; blue line, PtO_2; (b) black line, raw data; red line, Sn metal; green line, SnO_2.

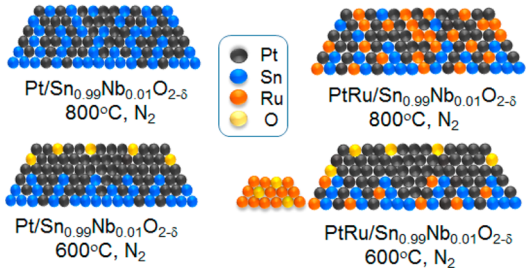

Figure 6. Schematic drawing of $PtRu/Sn_{0.99}Nb_{0.01}O_{2-\delta}$ and $Pt/Sn_{0.99}Nb_{0.01}O_{2-\delta}$ catalysts sintered at 600 and 800 °C under nitrogen atmosphere.

exposed on the top surface by sintering at 800 °C, and both catalysts reached the same order of $ECSA_{CO}$.

Figure 8 shows the hydrodynamic voltammograms for the oxidation of the methanol-formaldehyde mixtures for simulated fuels of POMM*n* (n = 2,3) on the various catalysts, $PtRu/Sn_{0.99}Nb_{0.01}O_{2-\delta}$, $Pt/Sn_{0.99}Nb_{0.01}O_{2-\delta}$, PtRu black, and Pt_2Ru_3/CB, in 0.1 mol dm^{-3} $HClO_4$ solutions saturated with oxygen at 25 °C. The current densities were calculated based on the geometric area. We found that the onset potentials (defined as the potential at which a current density of 10 $\mu A\ cm^{-2}$ was reached) of oxidation of the simulated fuels were less than 0.3 V vs RHE, which was more than 0.1 V lower than those of the commercial catalysts PtRu black and Pt_2Ru_3/CB. The mass activities (MA) for both $PtRu/Sn_{0.99}Nb_{0.01}O_{2-\delta}$ and $Pt/Sn_{0.99}Nb_{0.01}O_{2-\delta}$ at 0.45 V vs RHE were also improved with operating temperature (Figure 9), and reached values more

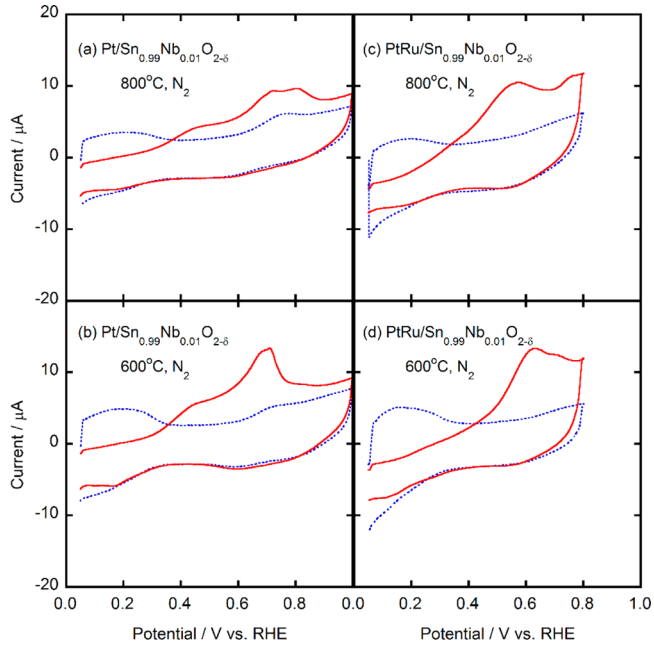

Figure 7. Adsorbed CO stripping voltammograms of (a) $Pt/Sn_{0.99}Nb_{0.01}O_{2-\delta}$ sintered at 600 °C, (b) $Pt/Sn_{0.99}Nb_{0.01}O_{2-\delta}$ sintered at 800 °C, (c) $PtRu/Sn_{0.99}Nb_{0.01}O_{2-\delta}$ sintered at 600 °C, (d) $PtRu/Sn_{0.99}Nb_{0.01}O_{2-\delta}$ sintered at 800 °C in 0.1 mol dm^{-3} $HClO_4$ solution saturated with N_2 at 25 °C. The dotted lines are the voltammograms obtained after CO stripping.

than 3 times larger than those for either PtRu black or Pt_2Ru_3/CB at 80 °C.

POMM*n* hydrolyzes promptly to formaldehyde and methanol under acid conditions and supplies protons via oxidation on the electrocatalyst (eqs 2–5).

$$C_{n+2}O_{n+1}H_{2n+6} + H_2O \rightarrow n\mathrm{HCHO} + 2CH_3OH \quad (2)$$

$$3Pt + \mathrm{HCHO} \rightarrow 2H - Pt + CO - Pt \quad (3)$$

$$5Pt + CH_3OH \rightarrow 4H - Pt + CO - Pt \quad (4)$$

$$H - Pt \rightarrow H^+ + e^- + Pt \quad (5)$$

The kinetics of oxidation for formaldehyde and methanol at the anode are strongly dependent on the poisoning of the intermediate carbon monoxide on the Pt surface (eqs 3 and 4). CO can be removed from the Pt surface by oxidation to CO_2. The adsorbed water on the Pt surface is the origin of atomic oxygen to oxidize the adsorbed CO on the Pt surface, but the CO easily adsorbs on the Pt surface and prevents the adsorption of water. The Pt alloying facilitates the oxidation of alcohols by shifting the onset of the reaction to less positive potentials. Typical alloying metals are Ru or Sn, which have a stronger affinity for the adsorption of atomic oxygen and water rather than CO, and can be act as supply sites for water and oxygen.

$$M + H_2O \rightarrow H_2O - M \quad (6)$$

$$H_2O - M + CO - Pt \rightarrow H - Pt + CO_2 \quad (7)$$

where M indicates either Ru or Sn. In the previous section, we explained that the top surface composition of Ru and Sn in each catalyst increased with increasing temperature. The presence of both elements on the top surface of catalyst would accelerate the CO oxidation reactions

dx.doi.org/10.1021/am505553b | ACS Appl. Mater. Interfaces 2014, 6, 22138–22145

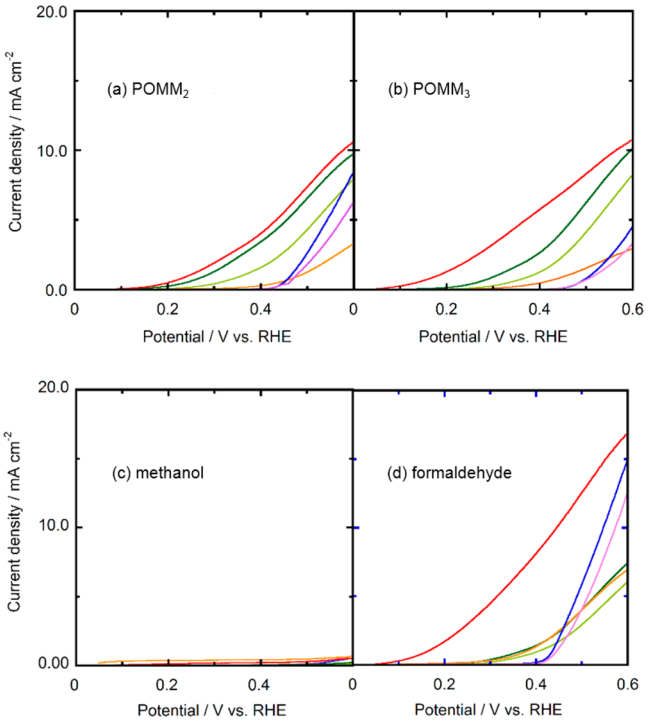

Figure 8. Hydrodynamic voltammograms for the oxidation of simulated fuels of both (a) $POMM_2$ and (b) $POMM_3$, (c) methanol and (d) formaldehyde on the various catalysts using the PtRu/$Sn_{0.99}Nb_{0.01}O_{2-\delta}$, Pt/$Sn_{0.99}Nb_{0.01}O_{2-\delta}$, Pt_2Ru_3/carbon black, and PtRu black at 25 °C. Blue line, Pt_2Ru_3/carbon black; violet line, PtRu black; orange line, PtRu/$Sn_{0.99}Nb_{0.01}O_{2-\delta}$ sintered at 600 °C under nitrogen atmosphere; red line, PtRu/$Sn_{0.99}Nb_{0.01}O_{2-\delta}$ sintered at 800 °C under nitrogen atmosphere; yellow-green line, Pt/$Sn_{0.99}Nb_{0.01}O_{2-\delta}$ sintered at 600 °C under nitrogen atmosphere; green line, Pt/$Sn_{0.99}Nb_{0.01}O_{2-\delta}$ sintered at 800 °C under nitrogen atmosphere.

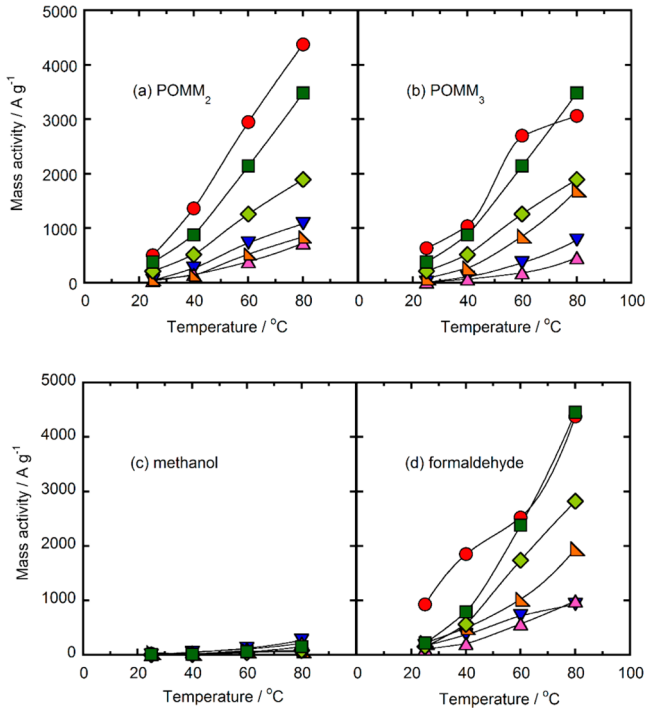

Figure 9. Mass activity for the oxidation of simulated fuels of both (a) $POMM_2$ and (b) $POMM_3$, (c) methanol, and (d) formaldehyde on the PtRu/$Sn_{0.99}Nb_{0.01}O_{2-\delta}$, Pt/$Sn_{0.99}Nb_{0.01}O_{2-\delta}$, PtRu black, and Pt_2Ru_3/CB as a function of temperature. Blue symbols, Pt_2Ru_3/carbon black; violet symbols, PtRu black; orange symbols, PtRu/$Sn_{0.99}Nb_{0.01}O_{2-\delta}$ sintered at 600 °C under nitrogen atmosphere; red symbols, PtRu/$Sn_{0.99}Nb_{0.01}O_{2-\delta}$ sintered at 800 °C under nitrogen atmosphere; yellow-green symbols, Pt/$Sn_{0.99}Nb_{0.01}O_{2-\delta}$ sintered at 600 °C under nitrogen atmosphere; green symbols, Pt/$Sn_{0.99}Nb_{0.01}O_{2-\delta}$ sintered at 800 °C under nitrogen atmosphere.

(eqs 6 and 7), and would improve the MA and onset potential.[12,13,35,36]

We also evaluated the oxidation reactions of methanol and formaldehyde, which can be obtained from the hydrolysis of POMM*n* (n = 2, 3) in acid media, on the various catalysts, Pt/$Sn_{0.99}Nb_{0.01}O_{2-\delta}$, PtRu/$Sn_{0.99}Nb_{0.01}O_{2-\delta}$, PtRu black, and Pt_2Ru_3/CB (Figure 8). The onset potentials for the methanol oxidation reaction (MOR) and the formaldehyde oxidation reaction (FOR) on both Pt/$Sn_{0.99}Nb_{0.01}O_{2-\delta}$ and PtRu/$Sn_{0.99}Nb_{0.01}O_{2-\delta}$ were less than those of the commercial catalyst PtRu black and Pt_2Ru_3/CB at 25 °C, and the potentials of these catalysts sintered at 800 °C were less than 0.2 V vs RHE. The MA values for the FOR at 0.45 V vs RHE for Pt/$Sn_{0.99}Nb_{0.01}O_{2-\delta}$ and PtRu/$Sn_{0.99}Nb_{0.01}O_{2-\delta}$ were improved with increasing operating temperature and reached values more than five times larger than those of the commercial catalysts at 80 °C (PtRu/$Sn_{0.99}Nb_{0.01}O_{2-\delta}$ sintered at 800 °C). The MA for the MOR at 0.45 V vs RHE for PtRu/$Sn_{0.99}Nb_{0.01}O_{2-\delta}$ and Pt/$Sn_{0.99}Nb_{0.01}O_{2-\delta}$ was as large as that of commercial Pt_2Ru_3/CB. (Figure 9). Each of the PtRu and Pt catalysts contained some Sn, as discussed in the previous section. The Sn is able to supply water or oxygen to the reaction sites on the Pt, which could be the origin of the improvement of the FOR and MOR via the bifunctional mechanism.[12,13,35,36] This enhancement of the activity of the catalyst helps to make the use of the POMM*n* fuels in DOFCs attractive from the viewpoint of performance and safety.

CONCLUSIONS

Pt and PtRu catalysts supported on Nb-doped $SnO_{2-\delta}$ (Pt/$Sn_{0.96}Nb_{0.04}O_{2-\delta}$, PtRu/$Sn_{0.99}Nb_{0.01}O_{2-\delta}$) were synthesized by the colloidal method for application as anodic catalysts for DOFCs. We found that the onset potentials of the oxidation reaction for simulated fuels of poly oxymethylene-dimethyl ether (POMM*n*, n = 2, 3) for Pt/$Sn_{0.99}Nb_{0.01}O_{2-\delta}$ and PtRu/$Sn_{0.99}Nb_{0.01}O_{2-\delta}$ were lower than those of the commercial catalysts PtRu black and Pt_2Ru_3/CB. In particular, the onset potential for PtRu/$Sn_{0.99}Nb_{0.01}O_{2-\delta}$ sintered at 800 °C reached values lower than 0.1 V vs RHE, which would enhance the operating voltage of the DOFC. The MA values of Pt/$Sn_{0.99}Nb_{0.01}O_{2-\delta}$ and PtRu/$Sn_{0.99}Nb_{0.01}O_{2-\delta}$ were also larger than those of the commercial catalysts in the measurement temperature range from 25 to 80 °C. In particular, the MA for the formaldehyde oxidation reaction on PtRu/$Sn_{0.99}Nb_{0.01}O_{2-\delta}$ sintered at 800 °C was more than five times larger than those of typical commercial catalysts over a range of temperatures, whereas the MA for the methanol oxidation reaction was unchanged.

All of the Pt and PtRu catalysts prepared in this study reacted with the $Sn_{0.99}Nb_{0.01}O_{2-\delta}$ support during the sintering procedure, and Sn diffused into the catalyst. Both Sn and Ru can adsorb water and thus accelerate the oxidation of CO on Pt, based on the bifunctional mechanism, which would accelerate the oxidation reaction activity of POMM*n* (n = 2, 3).

dx.doi.org/10.1021/am505553b | ACS Appl. Mater. Interfaces 2014, 6, 22138−22145

■ ASSOCIATED CONTENT

Supporting Information

The techniques for chemical composition analysis with STEM-EDX. This material is available free of charge via the Internet at http://pubs.acs.org.

■ AUTHOR INFORMATION

Corresponding Authors

*E-mail: kkakinuma@yamanashi.ac.jp. Tel.: +81 55 254 7143. Fax: +81 55 254 7143.

*E-mail: m-watanabe@yamanashi.ac.jp. Tel.: +81 55 254 7091. Fax: +81 55 254 7091.

*E-mail: uchidam@yamanashi.ac.jp. Tel.: +81-55-254-7095. Fax: +81-55-254-7095.

Present Address

§Graduate School of Science and Engineering, Yamaguchi University, 2-16-1, Tokiwadai, Ube 755-8611, Japan

Notes

The authors declare no competing financial interest.

■ ACKNOWLEDGMENTS

This work was partially supported by funds for the "Adaptable and Seamless Technology Transfer through Target-Driven R&D" Project (A-STEP) from the Japan Science and Technology Agency (JST), JSPS KAKENHI Grant B24350093 and the "Research on Nanotechnology for High Performance Fuel Cells (HiPer-FC)" project from the New Energy and Industrial Technology Development Organization (NEDO) of Japan.

■ REFERENCES

(1) Lamy, C.; Lima, A.; LeRhun, V.; Delime, F.; Coutanceau, C.; Legér, J.-M. Recent Advances in the Development of Direct Alcohol Fuel Cells (DAFC). *J. Power Sources* **2005**, *105*, 283−296.

(2) Rashidi, R.; Dincer, I.; Naterer, G. F.; Berg, P. Performance Evaluation of Direct Methanol Fuel Cells for Portable Applications. *J. Power Sources* **2009**, *187*, 509−516.

(3) Aricò, A. S.; Srinivasan, S.; Antonucci, V. DMFCs from Fundamental Aspects to Technology Development. *Fuel Cells* **2001**, *1*, 133−161.

(4) Hamnett, A. Mechanism and Electrocatalysis in the Direct Methanol Fuel Cell. *Catal. Today* **1997**, *38*, 445−457.

(5) Antolini, E. Catalysts for Direct Ethanol Fuel Cells. *J. Power Sources* **2007**, *170*, 1−12.

(6) Lamy, C.; Rousseau, S.; Belgsir, E. M.; Coutanceau, C.; Léger, J.-M. Recent Progress in the Direct Ethanol Fuel Cell: Development of New Platinum-Tin Electrocatalysts. *Electrochim. Acta* **2004**, *49*, 3901−3908.

(7) Cao, D.; Bergens, S. H. A Direct 2-Propanol Polymer Electrolyte Fuel Cell. *J. Power Sources* **2003**, *124*, 12−17.

(8) Qi, Z.; Kaufman, A. Performance of 2-Propanol in Direct-Oxidation Fuel Cells. *J. Power Sources* **2002**, *112*, 121−129.

(9) Vigier, F.; Coutanceau, C.; Léger, J. M.; Dubois, J. L. Polyoxymethylenedimethylether (CH_3-O-(CH_2-O)$_n$-CH_3) Oxidation on Pt and Pt/Ru Supported Catalysts. *J. Power Sources* **2008**, *175*, 82−90.

(10) Devaux, D.; Yano, H.; Uchida, H.; Dubois, J. L.; Watanabe, M. Electro-Oxidation of Hydrolysed Poly-Oxymethylene-Dimethylether on PtRu Supported Catalysts. *Electrochim. Acta* **2011**, *56*, 1460−1465.

(11) Baranton, S.; Uchida, H.; Tryk, D. A.; Dubois, J. L.; Watanabe, M. Hydrolyzed Polyoxymethylenedimethylethers as Liquid Fuels for Direct Oxidation Fuel Cells. *Electrochim. Acta* **2013**, *108*, 350−355.

(12) Watanabe, M.; Motoo, S. Electrocatalysis by Ad-Atoms: Part 2, Enhancement of the Oxidation of Methanol on Platinum by Ruthenium Ad-Atoms. *J. Electroanal. Chem. Interfacial Electrochem.* **1975**, *60*, 267−273.

(13) Watanabe, M.; Motoo, S. Electrocatalysis by Ad-Atoms: Part 3, Enhancement of the Oxidation of Carbon Monoxide on Platinum by Ruthenium Ad-Atoms. *J. Electroanal. Chem. Interfacial Electrochem.* **1975**, *60*, 275−283.

(14) Antolini, E. Formation of Carbon-Supported PtM Alloys for Low Temperature Fuel Cells: A Review. *Mater. Chem. Phys.* **2003**, *78*, 563−573.

(15) Jusys, Z.; Kaiser, J.; Behm, R. J. Composition and Activity of High Surface Area PtRu Catalysts towards Adsorbed CO and Methanol Electrooxidation-A DEMS Study. *Electrochim. Acta* **2002**, *47*, 3693−3706.

(16) Zhou, W. J.; Zhou, B.; Li, W. Z.; Zhou, Z. H.; Song, S. Q.; Sun, G. Q.; Xin, Q.; Douvartzides, S.; Goula, M.; Tsiakaras, P. Performance Comparison of Low-Temperature Direct Alcohol Fuel Cells with Different Anode Catalysts. *J. Power Sources* **2004**, *126*, 16−22.

(17) Neto, A. O.; Dias, R. R.; Tusi, M. M.; Linardi, M.; Spinaće, E. V. Electro-Oxidation of Methanol and Ethanol Using PtRu/C, PtSn/C and PtSnRu/C Electrocatalysts Prepared by an Alcohol-Reduction Process. *J. Power Sources* **2007**, *166*, 87−91.

(18) Chu, Y. H.; Shul, Y. G. Combinatorial Investigation of Pt-Ru-Sn Alloys as an Anode Electrocatalysts for Direct Alcohol Fuel Cells. *Int. J. Hydrogen Energy* **2010**, *35*, 11261−11270.

(19) Wang, D.; Lu, S.; Jiang, S. P. Tetrahydrofuran-Functionalized Multi-Walled Carbon Nanotubes as Effective Support for Pt and PtSn Electrocatalysts of Fuel Cells. *Electrochim. Acta* **2010**, *55*, 2964−2971.

(20) Zheng, L.; Xiong, L.; Liu, Q.; Han, K.; Liu, W.; Li, Y.; Tao, K.; Niu, L.; Yang, S.; Xia, J. Enhanced Electrocatalytic Activity for the Oxidation of Liquid Fuels on PtSn Nanoparticles. *Electrochim. Acta* **2011**, *56*, 9860−9867.

(21) Almeida, T. S.; Palma, L. M.; Leonello, P. H.; Morais, C.; Kokoh, K. B.; De Andrade, A. R. An Optimization Study of PtSn/C Catalysts Applied to Direct Ethanol Fuel Cell: Effect of the Preparation Method on the Electrocatalytic Activity of the Catalysts. *J. Power Sources* **2012**, *215*, 53−62.

(22) Nakagawa, N.; Ito, Y.; Tsujiguchi, T.; Ishitobi, H. Improved Reaction Kinetics and Selectivity by the TiO_2-Embedded Carbon Nanofiber Support for Electro-Oxidation of Ethanol on PtRu Nanoparticles. *J. Power Sources* **2014**, *248*, 330−336.

(23) Crisafulli, R.; Antoniassi, R. M.; Oliveira, N. A. Spinacé, E. V. Acid-Treated PtSn/C and PtSnCu/C Electrocatalysts for Ethanol Electro-Oxidation. *Int. J. Hydrogen Energy* **2014**, *39*, 5671−5677.

(24) Wang, Y.; Wu, G.; Wang, Y.; Wang, X. Effect of Water Content on the Ethanol Electro-Oxidation Activity of Pt-Sn/Graphene Catalysts Prepared by the Polyalcohol Method. *Electrochim. Acta* **2014**, *130*, 135−140.

(25) Kakinuma, K.; Uchida, M.; Kamino, T.; Uchida, H.; Watanabe, M. Synthesis and Electrochemical Characterization of Pt Catalyst Supported on $Sn_{0.96}Sb_{0.04}O_{2-\delta}$ with a Network Structure. *Electrochim. Acta* **2011**, *56*, 2881−2887.

(26) Kakinuma, K.; Chino, Y.; Senoo, Y.; Uchida, M.; Kamino, T.; Uchida, H.; Watanabe, M. Characterization of Pt Catalysts on Nb-Doped and Sb-Doped $SnO_{2-\delta}$ Support Materials with Aggregated Structure by Rotating Disk Electrode and Fuel Cell Measurement. *Electrochim. Acta* **2013**, *110*, 316−324.

(27) Senoo, Y.; Kakinuma, K.; Uchida, M.; Uchida, H.; Deki, S.; Watanabe, M. Improvements of Electrical and Electrochemical Properties at Nb-Doped $SnO_{2-\delta}$ Supports by Aggregation and Pt Loading as Fuel Cell Cathode Catalysts. *RSC Adv.* **2014**, *4*, 32180−32188.

(28) Yano, H.; Song, J. M.; Uchida, H.; Watanabe, M. Temperature Dependence of Oxygen Reduction Activity at Carbon-Supported Pt_xCo (x = 1, 2, and 3) Alloy Catalysts Prepared by the Nanocapsule Method. *J. Phys. Chem. C* **2008**, *112*, 8372−8380.

(29) Wakabayashi, N.; Takeichi, M.; Itagaki, M.; Uchida, H.; Watanabe, M. Temperature-Dependence of Oxygen Reduction Activity at a Platinum Electrode in an Acidic Electrolyte Solution Investigated with a Channel Flow Double Electrode. *J. Electroanal. Chem.* **2005**, *574*, 339−346.

(30) Higuchi, E.; Uchida, H.; Watanabe, M. Effect of Loading Level in Platinum-Dispersed Carbon Black Electrocatalysts on Oxygen Reduction Activity Evaluated by Rotating Disk Electrode. *J. Electroanal. Chem.* **2005**, *583*, 69−76.
(31) Watanabe, M.; Uchida, M.; Motoo, S. Preparation of Highly Dispersed Pt+Ru Alloy Clusters and the Activity for the Electrooxidation of Methanol. *J. Electroanal. Chem.* **1987**, *229*, 395−406.
(32) Uchida, M.; Aoyama, Y.; Eda, N.; Ohta, A. Investigation of the Microstructure in the Catalyst Layer and Effects of Both Perfluorosulfonate Ionomer and PTFE-Loaded Carbon on the Catalyst Layer of Polymer Electrolyte Fuel Cells. *J. Electrochem. Soc.* **1995**, *142*, 4143−4149.
(33) Uchida, M.; Fukuoka, Y.; Sugawara, Y.; Eda, N.; Ohta, A. Effects of Microstructure of Carbon Support in the Catalyst Layer on the Performance of Polymer-Electrolyte Fuel Cells. *J. Electrochem. Soc.* **1996**, *143*, 2245−2252.
(34) NIST X-ray Photoelectron Spectroscopy Database. http://srdata.nist.gov/xps/Default.aspx (accessed May 20, 2014).
(35) Motoo, S.; Watanabe, M. Electrocatalysis by Sn and Ge Ad-Atoms. *J. Electroanal. Chem.* **1976**, *69*, 429−431.
(36) Watanabe, M.; Furuuchi, Y.; Motoo, S. Electrocatalysis by Ad-Atoms Part XIII. Preparation of Ad-Electrodes with Tin Ad-Atoms for Methanol, Formaldehyde and Formic Acid Fuel Cells. *J. Electroanal. Chem.* **1985**, *191*, 367−375.